Defence Science Journal, Vol. 68, No. 6, November 2018, pp. 540-546, DOI : 10.14429/dsj.68.12731

Detection and Identification of Camouflaged Targets using Hyperspectral and LiDAR data

Deepti Yadav[#,*], M.K. Arora[#], K.C. Tiwari[@], and J.K. Ghosh[#]

[#]*Civil Engineering Department, Indian Institute of Technology, Roorkee, Roorkee - 247 667, India*
[@]*Department of Civil Engineering, Delhi Technological University, Delhi - 110 042, India*
[*]*E-mail: deepti.kanishk@gmail.com*

ABSTRACT

Camouflaging is the process of merging the target with the background with the aim to reduce/delay its detection. It can be done using different materials/methods such as camouflaging nets, paints. Defence applications often require quick detection of camouflaged targets in a dynamic battlefield scenario. Though HSI data may facilitate detection of camouflaged targets but detection gets complicated due to issues (spectral variability, dimensionality). This paper presents a framework for detection of camouflaged target that allows military analysts to coordinate and utilise the expert knowledge for resolving camouflaged targets using remotely sensed data. Desired camouflaged target (set of three chairs as a target under a camouflaging net) has been resolved in three steps: First, hyperspectral data processing helps to detect the locations of potential camouflaged targets. It narrows down the location of the potential camouflaged targets by detecting camouflaging net using Independent component analysis and spectral matching algorithms. Second, detection and identification have been performed using LiDAR point cloud classification and morphological analysis. HSI processing helps to discard the redundant majority of LiDAR point clouds and support detailed analysis of only the minute portion of the point cloud data the system deems relevant. This facilitates extraction of salient features of the potential camouflaged target. Lastly, the decisions obtained have been fused to infer the identity of the desired targets. The experimental results indicate that the proposed approach may be used to successfully resolve camouflaged target assuming some *a priori* knowledge about the morphology of targets likely to be present.

Keywords: Camouflaged target; ICA; HSI target detection; LiDAR classification; Decision level fusion

1. INTRODUCTION

Camouflaging is the concept that bears its origin from nature. This concept has been actively adopted and developed by humans particularly for defence applications, mainly for deceiving the enemy on battlefield. However, the battlefield today is now increasingly getting analysed using images acquired in different parts of the electro-magnetic (EM) spectrum[1]. Camouflaging too, therefore, aims at preventing detection of targets across different parts of EM spectrum using different techniques such as hiding, blending as summarised in Table 1[1].

Defence applications often require quick detection of camouflaged targets in a dynamic battlefield for an optimal allotment of limited resources. Additionally, military target detection puts very high qualitative demands[2,8]. Therefore, detection of the targets such as camouflaged military facilities/ uniforms is a challenging task[1]. Advancements in remote sensing data and technologies have greatly facilitated the detection of camouflaged targets in different regions of EM spectrum. These regions may be used either individually or collectively for detection of the camouflaged target. In particular, hyperspectral data, due to its high spectral resolution, offers an advantage of defeating camouflage[6]. Kim[6] states that a large number of spectral bands provided by hyperspectral imaging can support detection of camouflaged targets. It can be done by selecting suitable spectral bands which are capable of discriminating the camouflaged targets. Experiments considered hyperspectral data consisting of 1040 bands captured using a SPECIM_VNIR camera in 400 nm - 1000 nm range. He proposed a distance metric and an entropy-based spatial grouping method for selection of bands that support detection of camouflaged regions. The detection rate (DR) obtained using the *k*-means clustering algorithm demonstrated very high DR (99 per cent) in comparison to principal component analysis (DR = 92 %). Therefore, HSI appears to have the potential to support the detection of camouflaged targets[6,8,9]. However, background clutter, target-variability. under operational conditions can significantly degrade the accuracy of detection[8]. Further, the camouflaging process also adds to the existing target variability and thus may introduce more false alarms in detection. Therefore, detection of the camouflaged target using HSI is a challenging task[1,8,9].

Literature suggests that different datasets such as radio detection and ranging (RADAR), light detection and ranging

Received : 20 February 2018, Revised : 08 August 2018
Accepted : 28 August 2018, Online published : 31 October 2018

Table 1. Camouflaging materials

Camouflaging technique	EM Region		
	Optical	**IR/Thermal**	**Microwave**
Hiding	Earth-cover, vegetation net	Earth-cover, screens, smoke	Chaff, radar absorbing materials (RAM)
Blending	Paint, vegetation	Thermal paint, air conditioning	Vegetation RAM, reshaping, textured-mats
Disguising/disrupting	Reshaping, paint	Reshaping, paint	Reshaping corner reflectors

(LiDAR) provide uncorrelated information about the target and thus can aid in distinguishing the camouflaged target from its natural background[5,6]. Cheng[5], *et al.* proposed joint usage of visible images (captured at 555 nm) and near-infrared polarimetric images (captured at 750 nm) using polarised modified soil adjusted vegetation index for detection of the camouflaged target under vegetation environment. Results demonstrated that camouflaged target was well separated from the background. Several researchers have used HSI and LiDAR for detection of numerous man-made objects such as buildings, streets, tree-species identification using methods involving fusion, supervised/unsupervised classifications[6,7]. Thus, combined use of different kinds of data can achieve higher detection accuracies over the data used from a single sensor[8]. However, these approaches require the use of specialised sensors and thus making data acquisition expensive, and may also require additional processing such as spatial scaling. The background clutter may still have an effect on detection. Under these circumstances, shape-based methods may be useful for target identification[8]. Several shape-based methods *i.e.* rectangularity, contour-based models for target identification have been reported in the literature[9,10].

In this work, both spectral as well as shape information of targets have been used for detection and identification of camouflaged targets using HSI and LiDAR data. The work has been divided into two parts, first, detection of camouflaging material has been performed using spectral information from HSI data, which first has been pre-processed using independent component analysis (ICA). The pre-processing has assisted in selecting statistically independent components containing the camouflaging material[11]. ICA derived components were subjected to further detection processing. Next, identification of underlying camouflaged target has been performed using shape information from LiDAR data. Several approaches namely, contours, volumes, manual/expert analysis. have been used in several studies for identification of targets[12]. Here in light of *a priori* knowledge about potential target, few parameters namely DSM, alpha shape, height, and context. along with expert/ analyst knowledge have been used for inferring identification of potential target using LiDAR data[12]. Lastly, identity of the target has been confirmed using decision level fusion of results obtained from HSI and LiDAR data processing.

2. EXPERIMENTAL DATA

The data available for the study consisted of Hyperspectral and LiDAR data collected as part of a multimodal data collection campaign[13] conducted by Rochester Institute of Technology (RIT) in conjunction with SpecTIR, LLC, in the Rochester, New York, during July26-29, 2010.

2.1 Hyperspectral Data

The hyperspectral data has been captured using ProSpecTIR-VS2 in 360 bands ranging from 390 nm - 2450 nm with a spectral resolution of 10 nm and spatial resolution of 1 m, as shown in Fig. 1(a). For the purpose of the experiments, following two spatial subsets of this data have been used:

(i) Image-I refers to the first spatial subset of size 154 x 82 pixels (Fig. 1(b). It contains three camouflaging materials placed flat on road (*i.e.* green camouflaging-net (GREEN_CAMO), tan camouflaging-net (TAN_ CAMO) and three instance of green camouflaging-tarps (GREEN_TARP1-3), (Fig. 2(a)). They do not have any underlying target.

(ii) Image-II refers to the second spatial subset of size 67x42 pixels (Fig. 1(c)). This subset contains a camouflaging net (CAMO1) placed over a camouflaged target *i.e.* set of three chair (Fig. 2(b)).

2.2 LiDAR Data

Co-registered LiDAR data of same area has been collected using Leica ALS60. The spatial resolution of the LiDAR data is 1 m and its point density is 8 ppm. From this data, only one subset corresponding to the area covered by image-II has been generated for the purpose of experiments and referred to as LiDAR-II.

2.3 Ground Truth Data

Extensive ground truth data (ground photos, location (latitude and longitude) and high-resolution RGB ortho images as shown in Fig. 2 have also been also provided.

3. METHODOLOGY AND IMPLEMENTATION

The process of camouflaging makes detection of any target a challenging task by hiding the target under a camouflaging material. In this paper, an approach for detection and identification of a camouflaged target lying under camouflaging material has been evolved as shown in Fig. 3.

A two step-process has been adopted. First, camouflaging materials have been detected by implementing ICA on the hyperspectral data followed by applying matched filter (MF) and adaptive cosine estimator (ACE) algorithm on ICA derived components. The locations (latitude-longitude) of the pixels of camouflaging materials, thus identified, have been stored as seed locations of potential camouflaged target[15]. Second, LiDAR point cloud data has been classified into user-defined classes. Next, the shape of classes at the seed locations have been estimated using alpha shape and DSM. Several other information about targets such as its height, structure, and context have also been obtained using LiDAR data. Lastly, decisions obtained from HSI, LiDAR and morphological

(a)

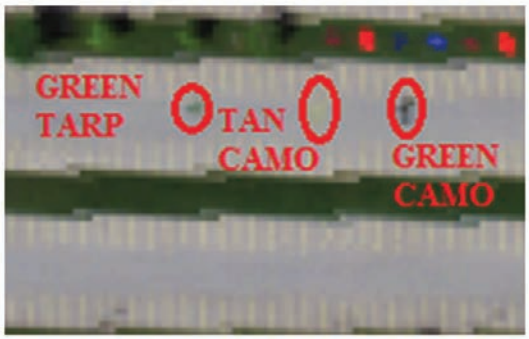

(b)

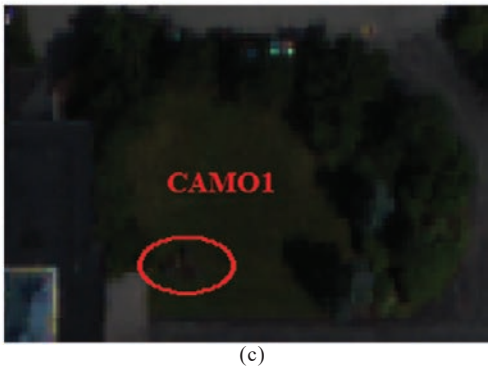

(c)

Figure 1. (a) Orthorectified true-color image of RIT-Campus and (b) Image-I, (c) Image-II

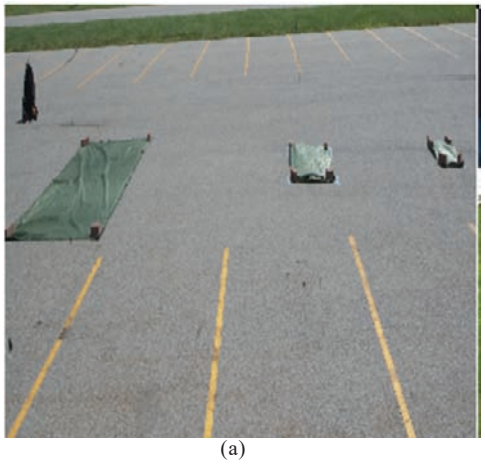

(a)

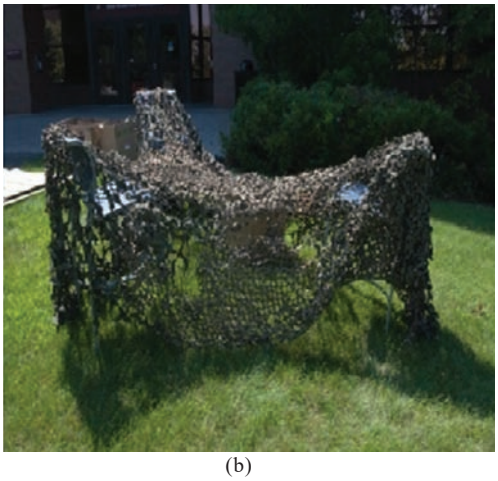

(b)

Figure 2. Ground photo (a) camouflaging material and (b) camouflaged target under CAMO1.

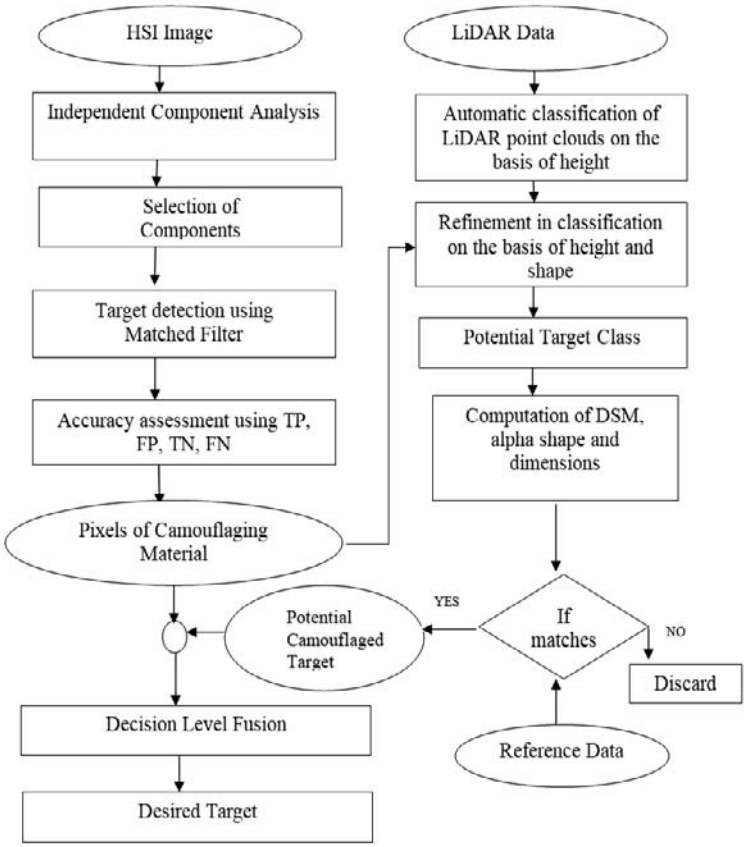

Figure 3. Workflow of the proposed camouflaged target detection approach.

analysis have been fused to infer the identity of desired targets[8].

3.1 HSI Processing

ICA is a blind source separation approach that decomposes a complex dataset into statistically separable components. In this paper, Negentropy based Fast ICA algorithm has been implemented to generate 360 components[11]. The first 100 components with higher values of kurtosis have been selected. Next for detection of camouflaging material, ACE and MF have been implemented on data without and with ICA-based pre-processing (50, 100 and 200 ICA components). Lastly, the accuracy of detection of camouflaging materials has been assessed by computing detection statistics namely true positives (TP), false negatives (FN), false positives (FP) and true negatives (TN). The statistics have been computed using windows of different sizes covering a small area around camouflaging materials only. No detection statistics have been computed for image-II because all the three chairs of the camouflaged target lie entirely within one pixel only.

3.2 LiDAR data processing

LiDAR data has been used to first detect the camouflaged target by classification of LiDAR point cloud and then perform identification using shape-based analysis of the detections obtained. LiDAR detection assumes that the user has some *a priori* knowledge about the morphology of the target. Initially, seven user-defined classes have been identified in the LiDAR data on the basis of knowledge about the presence of these features in image-II. These classes include ground, building, low/medium/high vegetation, road and potential target (set of three chairs). The LiDAR raw point-cloud data has been progressively classified into these seven classes on the basis of height, intensity, contextual information and 3-dimensional shape.

For classification, firstly points belonging to a ground class are separated from non-ground points using an algorithm based on progressive densification of triangulated irregular network (TIN) surfaces[14]. Second, all non-ground class points have been processed for finding points belonging to building class by finding points which along with its neighboring points form a planar surface with an area greater than a predetermined threshold and have single echo return. Next, remaining non-ground class points have been classified into vegetation classes (*i.e.* low/medium/high) using macros defined on the basis of height(0.001 m - 0.3 m in low-vegetation class, 0.3 m - 3 m to medium-vegetation and 3 m - 20 m into high-vegetation class). Further, height-based classification of vegetation-class may misclassify LiDAR points belonging to several man-made features like vehicles, road into vegetation class and thus need to be segregated. These points are further segregated into vehicle, road, and potential target class using features such as dimensions, intensity, shape and context information.

After classification, locations of points belonging to potential target class is compared with the seed locations of the potential targets obtained from HSI data. Targets at coincident locations have been considered as points of potential camouflaged target and thus have been used further for identification. Lastly, verification has been performed using LiDAR data and visible band images[12]. Different shape extraction approaches of the LiDAR point cloud, such as DSM and alpha shape have been employed to enhance the visualisation and interpretation of the potential target. Other information about the target such as height, structure, topological and contextual information has also been extracted from classified LiDAR data. These provide useful information for target recognition tasks[15]. Identification of the target requires manual user assessment with visible remote sensing images[15,3]. Therefore, all of the parameters obtained have been stored and analysed using *a priori* knowledge of the desired camouflaged target to infer the identity of the targets obtained.

3.3 Decision Level Fusion

In this study, hyperspectral and LiDAR data have been fused using decision level fusion for detection and identification of the desired camouflaged target. Literature suggests that the choice of fusion method is highly dependent on application and data being processed[16]. Here, decision level fusion has been used since it preserves the unique characteristics of both the datasets used i.e. LiDAR and HSI[16]. Despite disparities in both the datasets, decision level fusion allows independent decisions to be collectively used for confirming the identity of the desired target[16]. Mathematically, two sources of information *i.e. S*1(HSI) and *S*2 (LiDAR) have been used to obtain local decisions d_1 (on the basis of location and spectral identity) and d_2 (on the basis of 3-Dimensional view, shape, height and morphological information). Lastly, both of the local decisions have been fused to obtain overall-decision, $D = (d_1 \cup d_2)$ for confirming the identity of the target. Finally, location of identified camouflaged target from LiDAR point cloud has been matched with the georeferenced images for the purpose of accuracy assessment.

4. RESULT AND DISCUSSIONS

4.1 HSI Processing

(a) Image-I: The ICA resulted into 360 components. Few components containing target information (encircled) are as shown in Fig. 4(a). Next, MF and ACE are implemented for detection of camouflaging materials. The results obtained after applying MF are as shown in Fig. 4(b) and detections statistics for ACE and MF have been summarised in Table 2.

Following observations can be made from Fig. 4 and Table 2,

i. GREEN_CAMO: Most of the target pixels have been detected using both algorithms in all experiments with

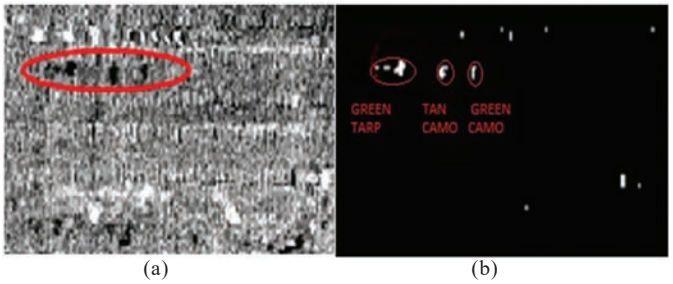

(a) (b)

Figure 4. Image-I results : (a) ICA component and (b) Binary image (detection for camouflaging-materials).

Table 2. Statistics for detection (camouflaging_Materials)

GREEN_CAMO (No. of Target-pixels:10)				
	ACE			
	ACE (No-ICA)	ACE (50-Component)	Proposed_Method (100-component)	ACE (200-Component)
TP	10	10	10	10
FN	0	0	0	0
FP	1889	330	88	250
TN	10729	12288	12530	12368
	MF			
	MF (No-ICA)	MF (50-component)	Proposed_Method (100-component)	MF (200-component)
TP	10	10	10	8
FN	0	0	0	2
FP	249	477	211	665
TN	12369	12141	12407	11953
TAN_CAMO (No. of target-pixels:16)				
	ACE			
	ACE (No-ICA)	ACE (50-component)	Proposed_Method (100-component)	ACE (200-Component)
TP	13	14	16	0
FN	3	2	0	16
FP	1	35	269	113
TN	12611	12577	12343	12499
	MF			
	MF (No-ICA)	MF (50-component)	Proposed_Method (100-component)	MF (200-component)
TP	13	16	14	13
FN	3	0	2	3
FP	211	344	60	458
TN	12401	12268	12552	12154
GREEN_TARP1(No. of target-pixels: 15)				
	ACE			
	ACE (No-ICA)	ACE (50-component)	Proposed_Method (100-component)	ACE (200-Component)
TP	13	14	15	2
FN	2	1	0	13
FP	161	239	53	541
TN	12452	12374	12560	12072
	MF			
	MF (No-ICA)	MF (50-component)	Proposed_Method (100-component)	MF (200-component)
TP	15	14	15	11
FN	0	1	0	4
FP	454	347	76	836
TN	12159	12266	12537	11777

TP>=8 out of 10.

ii. TAN_CAMO: Most of the target pixels have been detected using both algorithms in all of the four detection experiments with TP>=13 out of 16. MF performed better than ACE.

iii. GREEN_TARP1: Most of the target pixels have been detected. MF performs better than ACE (with 200 ICA component). However, Overall highest detection with lowest false alarms is produced by the proposed method.

(b) Image-II: Few of the ICA components generated using image-II are as shown in Fig. 5(a). Figure 5(b) shows detections obtained using MF on selected 100 ICA components.

It may be observed that MF, when applied on ICA components, leads to detection of pixels pertaining to camouflaging material CAMO1 (encircled and as shown in Fig. 5(b)) and several other pixels have also been detected as CAMO1. Here, detection statistics could not be computed since the size of the target (only one pixel) is very small with respect to spatial resolution. Next, all locations of the camouflaged material detected in image-II have been used as the seed locations of the potential camouflaged targets.

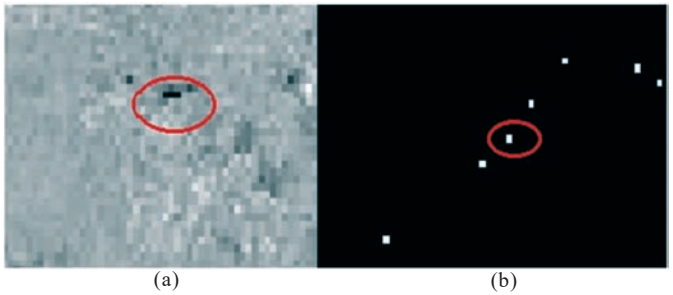

Figure 5. Image-II results (a) ICA component and (b) detection for CAMO1.

4.2 LiDAR Processing

The LiDAR point cloud has been classified into seven classes *i.e.* ground, building, vehicles, road, low/medium/high vegetation and potential target class based on height, intensity, contextual information, and shape, as shown in Fig. 6(a). Next, LiDAR points of potential target class have been processed further for identification, as shown in Fig. 7.

By comparing the shape of DSM (Fig. 7(c)) with the *a priori* known shape of the target (Fig. 7(a)), the camouflaged target can be visually identified. Additionally, three small peaks on the relatively flat ground can be observed from alpha-shape (Fig. 7(b)). These correspond to each of the three chairs in

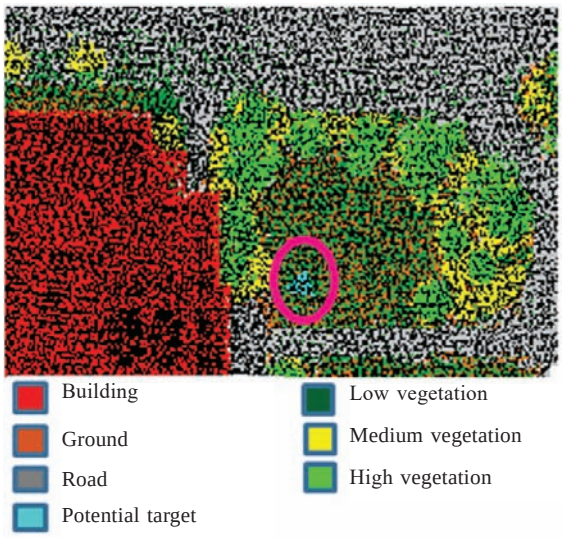

Figure 6. Classification of LiDAR point cloud (potential target encircled).

(a)

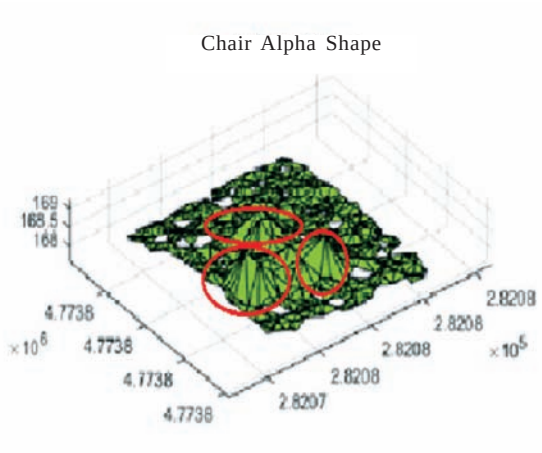

(b)

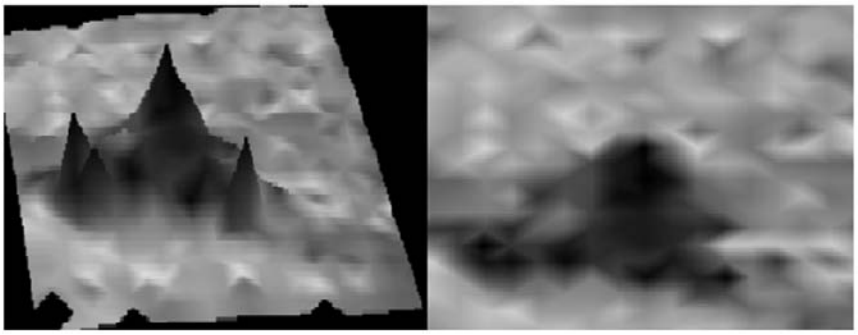

(c)

	Height (m)
Computed target	0.83, 0.79, 0.82 (height of three peaks)
Reference target	0.8

(d)

Figure 7. (a) Field photograph of camouflaged target, (b) Alpha-shape, (c) DSM (3D view and top-view), and (d) Height.

the desired camouflaged target being considered. Figure 7(d) summarises the approximate height measured for each of the peaks of the target and the referenced chair. Next as observed from classified point-cloud, the potential target has a volumetric structure and is placed perpendicularly on the ground without any trees or buildings in close proximity. Therefore on the basis of comparing the results obtained with visible images and *a priori* knowledge, and the target detected appears to be most likely the desired set of three camouflaged chairs.

Lastly, the identity of the potential target has been established using decision level fusion of spectral and shape information obtained from HSI and LiDAR analysis respectively. Therefore, combined decision $D = (d_1 \cup d_2)$ has been obtained by fusing

d_1= {Location, Spectral, Identity}, d_2= {3D shape, Alpha shape, Height, Contextual information, Exoert interpretation}

On comparison of *D* along with *a priori* knowledge about the target, potential target has been identified as a set of three chairs camouflaged under a net. Further, results obtained have been verified by comparing the locations of the detection with *a priori* known location of the targets which have been found to be almost similar (*i.e.* N 43 5 9.5, W 77 40 38.2 and N 43 5 9.3, W 77 40 38.4 respectively). Therefore, desired camouflaged target has been detected and identified by performing decision level fusion using hyperspectral and LiDAR data.

5. CONCLUSIONS

The paper presents a simple and efficient approach for fusion of hyperspectral and LiDAR data that can provide more situational awareness on the battlefield for detection and identification of camouflaged targets. Both spectral and shape information has been used for resolving camouflaged target hidden under camouflaging materials. Results demonstrate that detection of camouflaging material has been improved by performing ICA analysis prior to detection using MF and ACE. Lastly, identity of the target has been established by performing decision level fusion of spectral identity obtained using hyperspectral data and morphological identity obtained using LiDAR data. The benefit of shape information appears to be a promising way of improving spectral detection of targets in the real operational environment. In addition, the presented approach may also be used to reduce the massive amount of data generated from airborne LiDAR sensors into manageable relevant components which analysts can use to identify the desired camouflaged target. Future work may be directed towards establishing a quantitative method for comparing the shape of the detected target with a reference target.

REFERENCES

1. Wenshen, H.; Xun, L; & Yang, J. On combining spectral and spatial information of hyperspectral image for camouflaged target detecting. *In* International Conference on Optical Instruments and Technology: Optoelectronic Imaging and Processing Technology, SPIE-9045, 2013, 90451A1-8.
doi: 10.1117/12.2036546
2. Kim, S. & Shim, M. Cooperative spectral and spatial feature fusion for camouflaged target detection. *In* Algorithms and Technologies for Multispectral, Hyperspectral, and Ultraspectral Imagery XXI, SPIE, 2015, **9472**.

doi: 10.1117/12.2176979
3. Ratches, J. A. Review of current aided/automatic target acquisition technology for military target acquisition tasks. *Optical Engineering,* 2011, **50**(7), 072001-8. doi: 10.1117/1.3601879.
4. Murzina, M.V.A.; Farrell, J.P.; Aktsipetrov, O.A. & Murzina, T.V. Hyperspectral characterization of the adjustable nano-coating systems. *In* Non-destructive Detection and Measurement for Homeland Security III, SPIE, 2005, **5769**, 145-153. doi: 10.1117/12.598877
5. Cheng, Z. P.; Feng, W.; Kun, Z.H. & Mo-gen, X. Camouflaged target detection based on visible and near infrared polarimetric imagery fusion. *In* International Symposium on Photoelectronic_Detection_Imaging, SPIE, 2011, **8194**, 81940Y-7. doi: 10.1117/12.899590
6. Debes, C.; Merentitis, A.; Heremans, R.; Hahn, J.; Frangiadakis, N.; Kasteren T.V; Liao, W. & Bellens, R. Hyperspectral and LiDAR data fusion: Outcome of the 2013 GRSS data fusion contest. *IEEE J. Selected Topics Appl. Earth Obser. Remote Sens.,* 2014, **7**(6), 2405-2418. doi: 10.1109/JSTARS.2014.2305441
7. Zhang Q.;Pauca V. P.;Plemmons R. J. & Nikic D. D. Detecting objects under shadows by fusion of hyperspectral and lidar data: A physical model approach. *In* 5th Workshop Hyperspectral Image Signal Processing Evol. Remote Sensing (WHISPERS), 2013,1–4. doi: 10.1109/WHISPERS.2013.8080730
8. Bigdeli, B.; Samadzadegan, F. & Reinartz, P. Fusion of hyperspectral and LIDAR data using decision template-based fuzzy multiple classifier system. *Int. J. Appl. Earth Obser. Geoinfo.,* 2015, **38**, 309-320. doi: 10.1016/j.jag.2015.01.017
9. Li, Z.; Shi, W.; Wang, Q. & Miao, Z. Extracting man-made objects from high spatial resolution remote sensing images via fast level set evolutions. *IEEE Trans. Geosci. Remote Sens.,* 2015, **53**(2), 883-899. doi: 10.1109/TGRS.2014.2330341
10. Varney, N.M. & Asari, V.K. Volumetric features for object region classification in 3-D LiDAR point clouds. *In* Applied Imagery Pattern Recognition Workshop (AIPR), 2014, 1-6. doi: 10.1109/AIPR.2014.7041941
11. Tiwari, K.C.; Arora, M.K.; Singh, D. & Yadav, D. Military target detection using spectrally modeled algorithms and independent component analysis. *J. Optical Eng.,* 2013, **52**(2), 26402, 1-11. doi: 10.1117/1.OE.52.2.026402
12. Wang, S.; Hu, Q.; Wang, F.; Ai, M. & Zhong, R. A Microtopographic feature analysis-based LiDAR data processing approach for the identification of chu tombs. *Remote Sensing,* 2017, **9**(9), 880. doi: 10.3390/rs9090880
13. Herweg, J.A.; Kerekes, J.P.; Weatherbee, O.; Messinger, D.; Aardt, J.; Ientilucci, E.J.; Ninkov, Z.; Faulring, J.; Raqueño, N. & Meola, J. SpecTIR hyperspectral airborne rochester experiment data collection campaign. *In* Proceedings of Algorithms and Technologies for Multispectral, Hyperspectral, and Ultraspectral Imagery XVIII, SPIE, 2012, **8390**. doi: 10.1117/12.919268
14. Axelsson, P. DEM generation from laser scanner data using adaptive TIN models. *Int. Arch. Photogramm. Remote Sens.,* 2000, **33**, 111–118.
15. Guo, J.; Zhou, H. & Zhu, Ch. Cascaded classification of high-resolution remote sensing images using multiple contexts. *Inf. Sci.,* 2013, **221**, 84–97. doi: 10.1016/j.ins.2012.09.024
16. Bigdeli, B.; Samadzadegan, F. & Reinartz, P. Classifier fusion of hyperspectral and Lidar remote sensing data for improvement of land cover classification. *In* ISPRS-International Archives of the Photogrammetry, Remote Sensing and Spatial Information Sciences. XL-1/W3, 2013, 97-102. doi: 10.5194/isprsarchives-XL-1-W3-97-2013.

CONTRIBUTORS

Dr Deepti Yadav obtained her PhD from Indian Institute of Technology, Roorkee, India. Currently working as an Associate Professor in Department of Information Technology in Bharati Vidyapeeth's College of Engineering, Delhi, India. Her research interests include target detection in hyperspectral and multispectral data using digital image processing and soft techniques, remote sensing data fusion and analysis, GIS applications, machine learning.
In the current study, she designed and implemented the proposed approach for detection and identification of camouflaged target.

Prof. Manoj Kumar Arora is a Director at PEC University of Technology (on lien from Indian Institute of Technology, Roorkee, India). He is extremely experienced in optical remote sensing, in particular, hyperspectral imaging. His research interests include land cover mapping, digital image classification, neural networks and fuzzy logic, GIS and GPS applications, SAR interferometry, and landslide hazard studies.
In the current study, he guided the work and evaluated the results.

Prof. Kailash Chandra Tiwari is a Professor in the Department of Civil Engineering, Delhi Technological University, Delhi, India. He is an ex-army officer and his research interests primarily include detection of small and buried objects using microwave and hyperspectral remote sensing. His other areas of interest include detection in different bands of the electromagnetic spectrum, wave interaction with various media, and neural network applications in remote sensing. He has published more than 40 papers in Journals and Conference.
In the current study, he guided the work and evaluated the results.

Prof. Jayanta Kumar Ghosh is an Associate Professor in the Civil Engineering Department (Geomatics Engineering Group) of Indian Institute of Technology, Roorkee, India. He has more than 80 publications in the journals and conferences. He is a member of Institution of Engineers India, Indian National Cartographic Association, Indian Society of Remote Sensing, Institution of Navigation
In the current study, he guided the work and evaluated the results.